MOLECULAR & CELLULAR TOXICOLOGY, Vol. 2, No. 3, 216-221, September 2006

3D-QSAR Study of Competitive Inhibitor for Acethylcholine Esterase (AChE) Nerve Agent Toxicity

Amor A. San Juan[1,2] **& Seung Joo Cho**[1]

[1]Biochemicals Research Center, Korea Institute of Science and Technology, PO Box 131, Cheongryang, Seoul 130-650, South Korea
[2]University of Science and Technology, Daejeon 305-330, South Korea
Correspondence and requests for materials should be addressed to S.J. Cho (chosj@kist.re.kr)

Accepted 13 July 2006

Abstract

The cholinesterase-inhibiting organophosphorous (OP) compounds known as nerve agents are highly toxic. The principal toxic mechanism of OP compounds is the inhibition of acethylcholine esterase (AChE) by phosphorylation of its catalytic site. The reversible competitive inhibition of AChE may prevent the subsequent OP intoxication. In this study, three-dimensional quantitative structure-activity relationship (3D-QSAR) was performed to investigate the relationship between the 29 compounds with structural diversity and their bioactivities against AChE. In particular, predictive models were constructed using the comparative molecular field analysis (CoMFA) and comparative molecular similarity indices analysis (CoMSIA).

The results indicate reasonable model for CoMFA (q^2=0.453, r^2=0.697) and CoMSIA (q^2=0.518, r^2= 0.696). The presence of steric and hydophobic group at naphtyl moiety of the model may lead to the design of improved competitive inhibitors for organophosphorous intoxication.

Keywords: Acethylcholine esterase, Competitive inhibitors, CoMFA, CoMSIA, Nerve agent

The function of acethylcholine esterase (AChE) is to utilize acethylcholine through hydrolysis in cholinergic synapses[1]. AChE is a target enzyme for biologically active compounds including anti-Alzheimer disease agent[2], and warfare agents acting as reversible[3] or irreversible[4] inhibitors.

The most dangerous nerve agents[4] in chemical warfare are divided into two series. The G-series nerve agents include tabun, sarin (O-isopropyl methylphosphonofluoridate), soman (O-pinacolyl methylphosphonofluoridate), and cyclosarin while the V-series include VX (O-ethyl S-2-diisopropylaminoethyl-methyl phosphonothiolate). The two approaches to remedy the nerve agent poisoning involve the protection[3] of the AChE from phosphorylation by organophosphate (OP) compounds, or the reactivation[4] of the phosphylated AChE.

Each nerve agents contain OP moiety that binds irreversibly to AChE, which in effect causes human poisoning. To attenuate the toxicity caused by organophosphorous poisoning, reactivation process[5] should occur by hydrolytic cleavage of the organophosphoryl-AChE bond, or by dealkylation of the organophosphoryl-AChE complex. Organophosphorous-inhibited AChE can be reactivated by powerful nucleophiles like oxime[6]. Due to the different chemical structures of each nerve agents, their mechanism of action suggests differing rates of spontaneous reactivation. Non-spontaneous reactivation is noted for soman-AChE complex, with an aging half-life of about 2 min. On the other hand, a striking minimal percent reactivation (5%) is shown in sarin-AChE complex that is considered as the most dangerous organophosphorous agent.

The OP basic mechanism of action as it binds to AChE is based on the irreversible inhibition at cholinergic synapses. To protect the AChE from binding to OP, it appears that the first step of detoxification is by administering reversible AChE inhibitors to compete with the enzyme. The pre-treatment[3] against nerve agent enables the normal AChE to remain intact from OP irreversible inhibition. Subsequently, the AChE is recovered to perform its normal enzyme activity.

Both CoMSIA and CoMFA are 3D-QSAR techniques with different potential functions that describe the interaction between the ligand and the hypothesis receptor. The generated contour maps from 3D-QSAR models indicate the favorable and unfavorable fields for enhanced activity of the inhibitor. Thus, the combination of both techniques of 3D-QSAR analysis will give a comprehensive description for the reaction mechanism of the ligand-receptor interaction. One of the goals of this study is to discuss the interaction between the AChE and its competitive inhibitors by employing comparative molecular field analysis (CoMFA) and comparative molecular similarity indices analysis (CoMSIA). Furthermore,

Fig. 1. The alignment of the 29 AChE compounds by atom-atom fit.

the study aims to design potential competitive inhibitors for AChE.

The 3D-QSAR models were generated for a set of 29 structurally divergent AChE compounds. Using compound 20 as the template, the remaining compounds were aligned at a minimum energy conformation. Fig. 1 shows the 29 AChE compounds superimposed in their relative alignment. The relationship between the predicted and experimental activities for AChE showed low residuals (Table 2). The best predictions were obtained (Table 3) with CoMFA standard model (q^2=0.453, r^2=0.697) and with CoMSIA combined steric, electrostatic, hydrophobic and hydrogen bond acceptor fields (q^2=0.518, r^2=0.696). The

Table 1. The chemical structures and inhibition data for series of AChE compounds.

Series 1

Compound	R	IC_{50} (μM)
1	CH_3	290
2	$CH(CH_3)_2$	80
3	$CH_2C(CH_2)_3$	12
4	$CH(CH_3)C(CH_3)_3$	16
5	$(CH_2)_3CH_3$	20
6	$(CH_2)_7CH_3$	7
7	$CH_2C_6H_5$	50
8	$(CH_2)_3C_6H_5$	15
9	$CH_2C_{10}H_7$	7
10		340

Series 2

Compound	R	IC_{50} (μM)
11	(1,3,5 oxadiazole)CH_3	250
12	(1,3,5 oxadiazole)C_6H_5	22
13	(1,2,4 oxadiazole)C_6H_5	7.5
14	(1,2,4 oxadiazole)CH_3	310

Series 3

Compound	R	IC_{50} (μM)
15	C_6H_5	7.5
16	t-C_4H_9	99
17	n-$(CH_2)_7CH_3$	1.4
18	CH_3	104
19	L-naphthyl	1.3
20	$CH_2C_6H_5$	55
21	C_6H_5	220
22		890

Series 4

Compound	R	IC_{50} (μM)
23	Br	210
24		710
25	OCH_3	260
26	Cl	520
27	F	720
28	CN	180
29	Cl	330

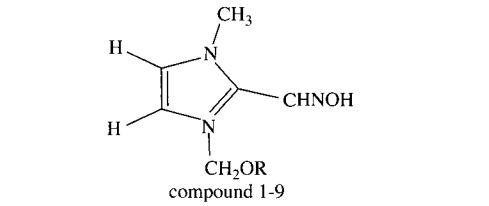

compound 1-9

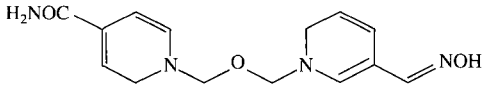

compound 10

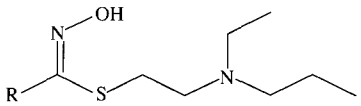

compounds 11-14

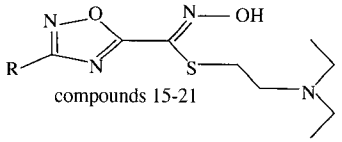

compounds 15-21

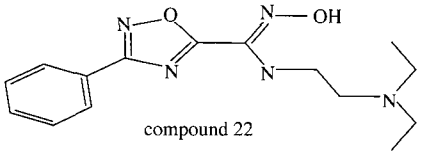

compound 22

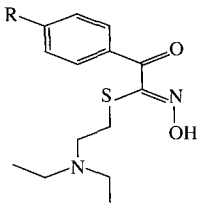

compounds 23-28

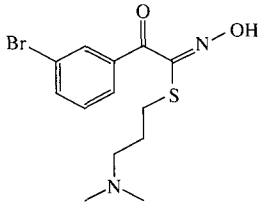

compound 24

Table 2. Predicted activities (PA) versus experimental activities (pIC_{50}) with residuals by CoMFA and CoMSIA analysis.

Compound	pIC_{50}	FleXx energy kcal.mol^{-1}	CoMFA		CoMSIA	
			PA	Residual	PA	Residual
Training						
3	−1.08	−8.9	−1.08	0.00	−1.06	−0.02
4	−1.20	−7.9	−1.20	0.00	−1.02	−0.18
5	−1.30	−9.4	−1.30	0.00	−1.14	−0.16
6	−0.84	−9.4	−1.19	0.35	−1.00	0.16
8	−1.18	−10.7	−1.32	0.14	−1.07	−0.11
9	−0.84	−12.5	−1.17	0.33	−1.21	0.37
12	−1.34	−14.0	−1.47	0.13	−1.68	0.34
13	−0.88	−14.0	−1.75	0.88	−2.09	1.22
15	−0.88	−13.3	−1.75	0.88	−2.09	1.22
16	−2.00	−2.8	−1.37	−0.63	−1.49	−0.51
17	−0.15	−7.7	−1.57	1.42	−1.43	1.28
18	−2.02	−18.9	−1.58	−0.44	−1.57	−0.45
19	−0.11	−15.1	−1.44	1.33	−1.53	1.42
21	−2.34	−13.2	−1.45	−0.89	−1.70	−0.64
23	−2.32	−16.6	−2.56	0.24	−2.56	0.24
24	−2.85	−17.0	−2.43	−0.42	−2.48	−0.37
25	−2.42	−15.0	−2.65	0.23	−2.41	−0.01
26	−2.72	−16.5	−2.64	−0.08	−2.54	−0.18
27	−2.86	−16.1	−2.61	−0.25	−2.49	−0.37
28	−2.26	−15.7	−2.67	0.42	−2.49	0.24
29	−2.52	−15.2	−2.56	0.04	−2.54	0.02
30	−1.34	−6.0	−1.34	0.00	−1.00	−0.34
31	−1.34	−9.7	−1.26	−0.08	−1.14	−0.20
32	−1.20	−6.8	−1.20	0.00	−0.96	−0.24
33	−0.70	−9.0	−1.18	0.48	−1.01	0.32
34	−1.11	−10.9	−0.76	−0.35	−1.02	−0.10
35	−0.85	−10.1	−0.78	−0.06	−1.19	0.34
36	−1.18	−0.7	−0.93	−0.25	−1.06	−0.11
40	−0.95	−6.1	−0.75	−0.20	−0.96	0.01
Test						
1	−2.46	−11.1	−1.13	−1.34	−1.13	−1.33
2	−1.90	−10.1	−1.24	−0.66	−1.19	−0.72
7	−1.70	−10.7	−1.25	−0.45	−1.11	−0.59
10	−2.53	−18.7	−1.26	−1.27	−1.21	−1.32
11	−2.40	−15.9	−1.78	−0.62	−1.78	−0.62
14	−2.49	−18.3	−1.54	−0.95	−1.57	−0.92
20	−1.74	−11.3	−1.45	−0.29	−1.54	−0.20
22	−2.95	−16.3	−1.51	−1.44	−1.36	−1.59
37	−1.61	−10.2	−1.03	−0.58	−1.15	−0.46
38	−1.79	−6.5	−0.88	−0.91	−1.18	−0.61
39	−1.11	−11.1	−0.87	−0.24	−1.09	−0.02

PLS analysis indicates that the combined CoMSIA model (steric, electrostatic, hydrophobic, hydrogen acceptor) have reasonable predictability. In regard to the low q^2 value obtained from CoMFA steric and electrostatic models, the result indicates that the model is not stable, possibly because of the high collinearity of each variable[11]. Therefore, the steric and electrostatic effects of a reversible inhibitor may be of less importance in the interaction between the AChE and its competitive inhibitor. In addition, the PLS analysis of CoMSIA implies that the hydrophobic and hydrogen acceptor models have a high statistic significance (q^2 is 0.518).

A potential competitive inhibitor for AChE may keep the enzyme active by making it unavailable for reaction with OP. The analogous binding between compound 20 to AChE (Fig. 2) as compared to the AChE-OP (Fig. 3) complex, may suggests that competitive inhibition shall thwart the irreversible binding of AChE-OP adduct. The irreversible OP-AChE inhibited enzyme shows a remarkable array of non-covalent bonds which is a charàcteristic of OP nerve agents. A molecular modeling retrospective study of the soman-AChE irreversible binding agrees

Table 3. Summary of results from CoMFA and CoMSIA analyses[a].

	CoMFA	CoMSIA		
	SE	SE	SE & H & DA	SD & H
		Statistical Result		
q^2	0.51	0.66	0.41	0.63
r^2	0.69	0.98	0.76	0.99
F	29.38	96.59	40.35	248.75
N	2	10	2	10
pred r^2	0.46			0.51
		Fraction (%)		
steric	0.69	0.73	0.17	0.32
electrostatic	0.32	0.27	0.17	
hydrophobic			0.26	0.41
donor			0.18	0.27
acceptor			0.22	

[a]SE: steric and electrostatic fields; DA: hydrogen donor and hydrogen acceptor fields; SD: steric and donor fields; H: hydrophobic field; q^2: Leave one out (LOO) cross-validated correlation coefficient; N: optimum number of components, r^2: noncross-validated correlation coefficient; F: value of F-test; pred r^2: predictive r^2

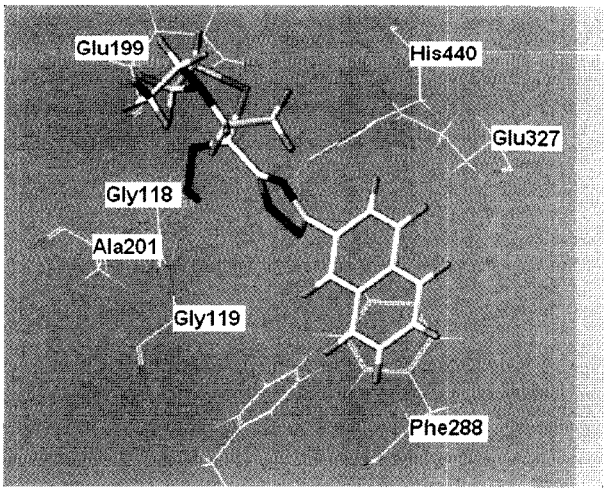

Fig. 2. Three hydrogen bonds formed at the oxyanion site of AChE bound to the most potent inhibitor (compound 20).

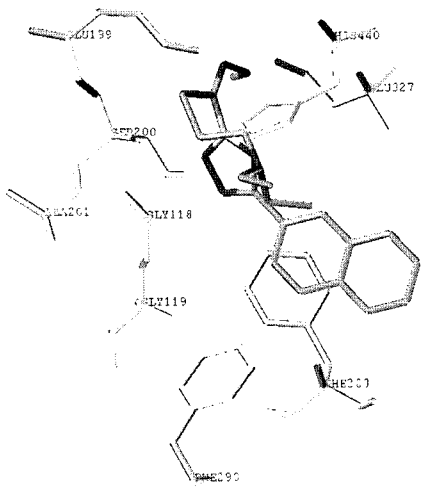

Fig. 3. Three hydrogen bonds formed at the oxyanion site of AChE bound to the most potent inhibitor (compound 19).

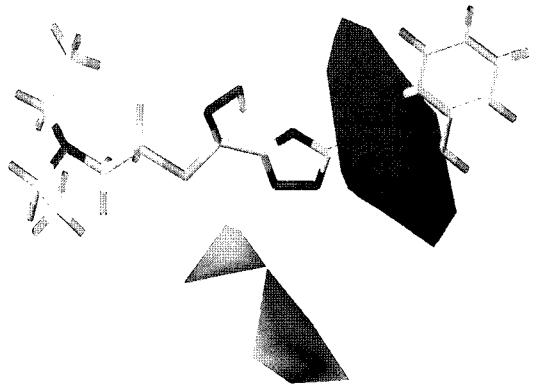

Fig. 4. CoMFA steric contour plot. Sterically favored areas (contribution level of 90%) are represented by green polyhedra. Sterically disfavored areas (contribution level 10%) are shown by yellow polyhedra.

with the three-dimensional crystal structure data[12], see Fig. 3 respectively. There are three strong hydrogen bonds formed from the oxyanion hole (Gly118, Gly119 and Glu199) to one of the phosphonyl oxygen atom of soman, in effect it stabilize the bound complex during the process of irreversible inhibition.

On the basis of interatomic interactions previously explained, the analysis of the structural features of the ligands potent activity to AChE is explained in the following 3D-QSAR results. Fig. 4 shows the CoMFA steric contour map, suggesting that the presence of methyl chains and bulky groups surrounding the oxadiazol moiety would disfavor the compound competitive binding to AChE-OP inhibited complex. Otherwise, a steric group along the naphthyl ring would enhance inhibition of AChE. Fig. 5 depicts the CoMFA electrostatic contour map implying that the presence of electronegative charge group located near the naphthyl ring and thiocarboxymic moieties would favor binding to AChE protein. Fig. 6 displays the hydrophobic contour map (on the basis of combined steric, electrostatic, hydrophobic and acceptor fields). The yellow color region located at the oxadiazole ring and part of naphthyl

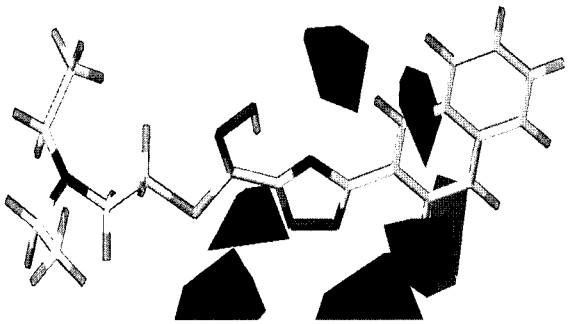

Fig. 5. CoMFA electrostatic contour plot. Positive charged favored areas (contribution level of 90%) are represented by blue polyhedra. Negative charged disfavored areas (contribution level 10%) are shown by red polyhedra.

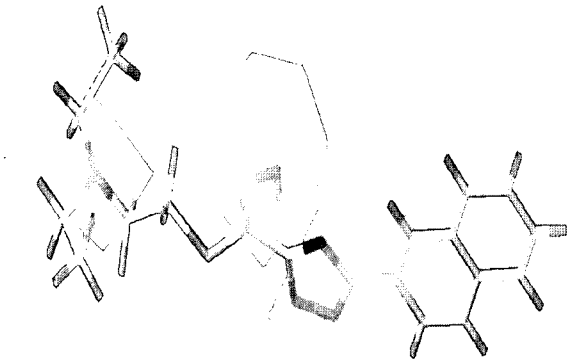

Fig. 6. CoMSIA combined hydrophobic contour plot. Hydrophobically favored areas (contribution level of 90%) are represented by yellow polyhedra. Hydrophobically disfavored areas (contribution level 10%) are shown by white polyhedra.

moiety suggests that the substitution by a hydrophobic group would decrease the activity. However, the attachment of hydrophobic group located near the hydroxyl moiety as well as tert-amine moieties would enhance the activity.

Discussion

The prevention of AChE toxicity can be avoided by the binding of a competitive reversible inhibitor to the enzyme. In this study, a new potential competitive inhibitor to AChE was designed by employing 3D-QSAR. The CoMFA and CoMSIA contour maps were utilized to analyze the structural features of the ligands accounting to the competitive inhibition towards the phosphonylated AChE. A compound with the presence of hydrophobic and electronegative groups to naphthyl moiety would enhance activity potency. Moreover, the presence of lipophilic group adjoining the oxadiazol and naphthyl part is expected to increase its binding affinity to the AChE. The characteristic of steric and electrostatic interactions have minor influence on the competitive inhibition to AChE.

Methods

The input structural data employed in the 3D-QSAR analysis consists of series AChE compounds, published by Bedford *et al.*[5-8]. The chemical structures and inhibition data of AChE inhibitors is shown in Table 1. The biochemical assay study contains 29 compounds with IC_{50} values within the range of 7 to 890 μM. Out of the 29 compounds, there were eight test set (compounds 1, 2, 7, 10, 11, 14, 20, and 22) selected, whereas the remaining 21 compounds were the training set.

Molecular modeling calculations were performed using SYBYL[9] program version 7.1 on silicon graphics origin300 workstation with IRIX 6.5 operating system. Energy minimizations of compounds were accomplished by assigning Tripos force field and Gasteiger charges at convergence criterion of 0.005 $kcal.mol^{-1}$. A bioactive conformation was chosen carefully to obtain a suitable conformational template for all the compounds. In this study, active analogue approach was executed to obtain bioactive conformation since there is no available crystal structure for the AChE-ligand complex. The alignment required in CoMFA was performed by atom-atom fit superposition method. Partial least squares (PLS) technique was employed for all 3D-QSAR modeling studies to relate linearly the descriptor fields with the inhibition values of the compounds. The CoMFA and CoMSIA descriptors were used as independent variables while the pIC_{50} values were utilized as dependent variables in PLS analyses to derive 3D-QSAR models. Initially, the predictability of the models was determined by leave-one-out (LOO)[10] cross-validation. Subsequently, to maintain the optimum number of PLS components and minimize the tendency to over fit the data, the number of components corresponding to the lowest PRESS value was employed to obtain the final PLS regression models.

Acknowledgements

The study was supported by a research grant from Korea Research Foundation.

References

1. Nachmansohn, D. Role of acetylcholine in neuromuscular transmission. *Proc. Natl. Acad. Sci. U.S.* **135**(1), 136-149 (1966).
2. Bai, D., Tang, X., He, X. & Huperzine, A. A potential therapeutic agent for treatment of Alzheimer's disease. *Curr. Med. Chem.* **7**(3), 355-374 (2002).
3. Bajgar, J. Prophylaxis against organophosphorous poisoning. *J. Med. Chem. Def.* **1**, 1-16 (2004).
4. Kassa, J. Review of oximes in the antidotal treatment of poisoning by organophosphorous nerve agents. *J. Toxicol.: Clin. Toxicol.* **40**, 803-816 (2002).
5. Bedford, C. *et al.* Structure-activity activity relationships for reactivators of organophosphorous-inhibited acethylcholinesterase: Quaternary salts of 2-[(hydroxyimino)methyl]imidazole. *J. Med. Chem.* **27**, 1431-1438 (1984).
6. Kenley, R. *et al.* Nonquaternary cholinesterase reactivators. 2. α-heteroaromatic aldoximes and thiohydroximates as reactivators of ethyl methylphosphonyl-acethylcholinesterase in vitro. *J. Med. Chem.* **27**, 1201-1211 (1984).
7. Bedford, C. *et al.* Nonquaternary cholinesterase reactivators. 3. 3(5)-substituted 1, 2, 4-oxadiazol-5(3)-aldoximes and 1, 2, 4-oxadiazole-5(3)-thiocarbohydroximates as reactivators of organophosphate-inhibited eel and human acethylcholinesterase in vitro. *J. Med. Chem.* **29**, 2174-2183 (1986).
8. Bedford, C. *et al.* Nonquaternary cholinesterase reactivators. 4. dialkylaminoalkyl thioesters of α-keto thiohydroximic acids as reactivators of ethyl methylphosphonyl- and 1, 2, 2-trimethylpropyl methylphosphonyl-acethylcholinesterase in vitro. *J. Med. Chem.* **29**, 1689-1696 (1986).
9. SYBYL 7.0 (2004) Tripos Inc., 1699 Hanley Road, St. Louis, MO 63144
10. Cramer, R.D.III, Bunce, J.D. & Patterson, D.E. Crossvalidation, bootstrapping, and partial least squares compared with multiple regression in conventional QSAR studies. Quant. Struct. *Act. Relat.* **7**, 18-25 (1998).
11. Golbraikh, A. & Tropsha, A. Beware of q^2! *J. Mol. Graph. Model.* **20**, 269-276 (2002).
12. Millard, C. *et al.* Reactivation products of acethylcholine and VX reveal a mobile histidine in the catalytic triad. *J. Am. Chem. Soc.* **121**, 9883-9884 (1999).